

**Ground-state configurations of ionic species I through XVI  
for  $Z=57-74$  and the interpretation of  $4d-4f$  emission  
resonances in laser-produced plasmas**

P.K. Carroll and G. O'Sullivan

*Physics Department, University College Dublin, Belfield, Dublin, Ireland*

(Received 11 September 1980; revised manuscript received 23 July 1981)

Spectra of the elements barium ( $Z=56$ ) through Nd ( $Z=60$ ) observed in laser-produced plasmas from pure-metal targets in the wavelength region 70–130 Å are presented. This completes our survey of the spectra of elements from cesium to hafnium in two regimes of optical thickness. The two sets of spectra show significant differences. In order to interpret the whole range of results, we need to know the ground-state configurations of ions in stages up to XVI for  $Z=55-71$ . From the limited-term analyses available, a table of plausible ground configurations is proposed. In the preparation of the table, the effect of increasing ionization, for a fixed  $Z$ , on wave-function contraction is studied, and it is inferred that the  $4f$  electron becomes more tightly bound than  $5p$  between the sixth and seventh spectra of the elements from cerium to lutetium; similarly the  $4f$  electron attains a higher binding energy than does the  $5s$  between the fourteenth and fifteenth spectra. Consequently, for a considerable range of ion stages, particularly in the rare earths, the ground configurations have a partially filled  $4f$  shell. Furthermore, in the same ion stages, the  $4f$ ,  $5p$ , and  $5s$  energies stay relatively close together so that configurations of the type  $5p^l 4f^{n-l}$  lie very near the nominal ground configuration. A corresponding manifold of overlapping excited configurations of the type  $4d^9 4f^{n+1}$ ,  $4d^9 5p^l 4f^{n-l+1}$  is also expected and the observed resonances arise from all of the  $4d-4f$  transitions permitted between the upper and lower manifolds of configurations. The numbers of transitions are calculated and in the majority of cases are very great. Because the principal quantum number does not change, the transitions will tend to overlap for different ion stages of any one element. The widths and varying complexity of the resonances can be explained in a satisfactory, if qualitative, way by means of available theory. The very considerable difference between the compound and metal spectra can be explained in terms of the effect of number density of the active species on both emission and absorption processes in the two types of plasma.

## I. INTRODUCTION

Recently, the observation of intense resonance-like emission features in the spectra of laser-produced plasmas of the elements from Cs to Yb has been reported.<sup>1</sup> The resonances lie in the 120–50 Å region, have a width of  $\sim 15$  eV, and move towards shorter wavelengths with increasing  $Z$ . In the low- $Z$  elements the resonances contain a number of strong lines, the intensity of which decreases along the sequence until the structure eventually becomes continuumlike. In each case, the targets employed contained only a small quantity of the element under investigation typical concentrations being  $\sim 1\%$ . Away from the resonances a few weak lines were observed (for the low- $Z$  elements only) and the background continuum was

extremely weak in every case.

In contrast, spectra of pure metal targets of the elements from Sm through Yb are known to yield essentially line-free continua throughout the entire spectral region from 40–2000 Å.<sup>2,3</sup> However, some modulation of these continua was observed for each element in the vicinity of the resonances, though the characteristic widths and profiles were very different. Again, however, the modulation diminished with increasing  $Z$ .

In order to interpret the observed trends, it seemed desirable to have data on the earlier elements (metals) of the sequence. A systematic study of the elements from Ba to Nd was therefore undertaken and yielded much more pronounced and structured modulations than in the case of the higher rare earths. Again, they were obviously re-

lated to the resonances observed in compounds but differed markedly in width, profile, and line density. These results, which constitute the experimental section of the present paper, complete our survey of the lanthanides and adjacent related elements as observed in laser-produced plasmas.

To account for the wealth of new experimental data now available, a knowledge of the electronic structure of elements from cesium to ytterbium is necessary. Since plasma considerations indicate that high ion stages are involved in the emission, the electron configurations of the relevant ground states must be known before a beginning can be made to interpreting the spectra. Unfortunately, for the species of interest, identifications of ground states are almost completely lacking. In the present paper, the problem of assigning ground configurations is discussed and the conclusions are summarized in the form of a table covering a considerable range of ion stages.

The trend of the energies of the relevant excited configurations is also analyzed. On the basis of these configuration studies, both types of resonance can be explained in a qualitative but quite detailed way.

## II. EXPERIMENTAL AND RESULTS

The experimental procedures have already been described in detail elsewhere.<sup>1</sup> A *Q*-switched ruby laser having an output of 1 J was used to generate the plasmas. The spectra were photographed on a 2-m grazing incidence vacuum spectrograph which had as dispersing element a Bausch and Lomb diffraction grating with 1200 rulings/mm. Traces of the spectra of the metals barium ( $Z=56$ ) through neodymium ( $Z=60$ ) in the region of interest are shown in Fig. 1. The spectrum of europium ( $Z=63$ ) is also included to show the trend towards continuumlike character with increasing atomic number. Spectra of the corresponding elements in compound form are displayed for comparison in Fig. 2. In the case of the compounds, the resonance is relatively narrow and extends typically over 8–18 eV. In the pure metal, on the other hand, the resonance extends to considerably longer wavelengths and covers an energy region of 30 eV. Towards the center of the resonance a pronounced minimum is evident.

## III. MAPPING OF GROUND-STATE CONFIGURATIONS

The behavior of the  $4f$  electron is crucial for an understanding of the ground-state configurations

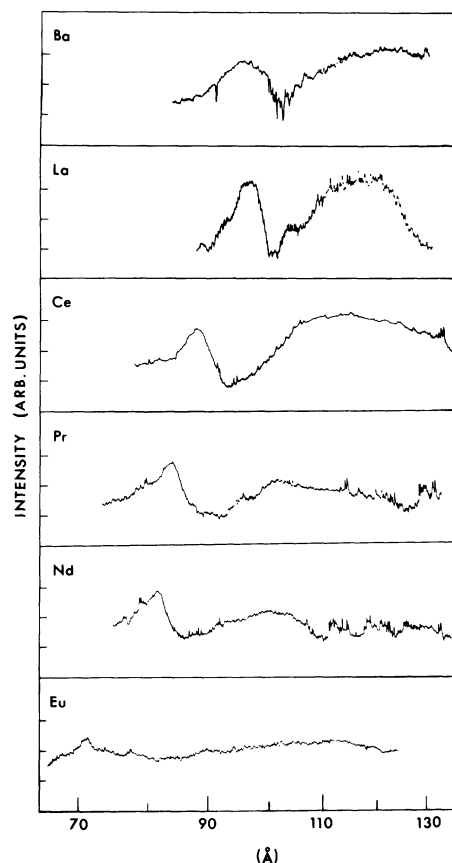


FIG. 1. Densitometer traces of spectra of elements Ba, La, Ce, Pr, Nd, and Eu obtained from laser plasmas generated on pure-metal targets.

of the lanthanides in their various stages of ionization. This behavior is well documented for the neutral atoms and their first few ion stages. We begin therefore by showing in the left-hand columns of Table I the configurations given by Martin *et al.*<sup>4</sup> for lanthanum through lutetium. Here it is seen that at the fourth spectrum the  $4f$  level has in all cases fallen below  $5d$  and  $6s$ . This is due to the well-known phenomenon of  $4f$  wavefunction collapse.<sup>5</sup> The effective potential in which the  $4f$  electron moves is made up of an attractive Coulomb term and a repulsive centrifugal term, which, in general, combine to give a double well potential, the height of the intervening barrier depending on the nuclear charge  $Z$ . For neutral atoms the field in the region of the outer potential is essentially hydrogenic. The occurrence of the neutral lanthanides coincides with the appearance of bound  $4f$  levels in the inner well, which, in turn, is due to the deepening of the well and the lowering of the potential barrier as a result of the in-

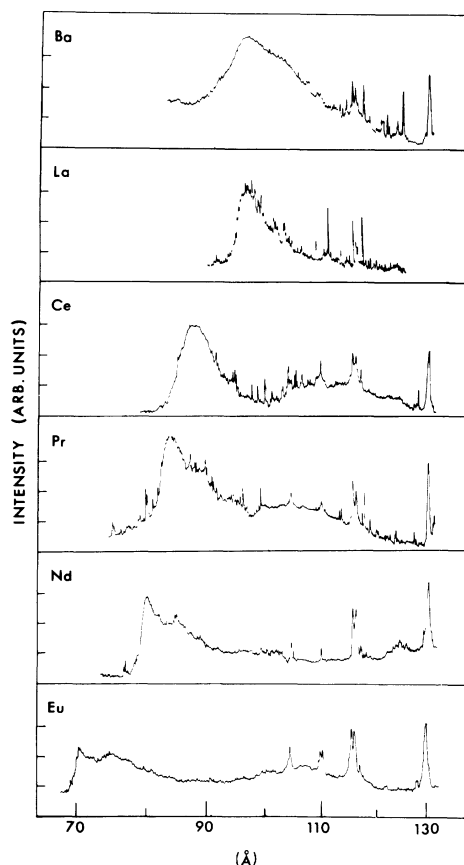


FIG. 2. Densitometer traces of spectra of the elements in Fig. 1, Ba, La, Ce, Pr, Nd, and Eu, obtained from compounds.

creasing nuclear charge.

Information on the ground states of higher ion stages is very limited. Direct observations for free ions are available only for those elements to the left of the full line in Table I and for members of the silver and palladium isoelectronic sequences shown on the right.<sup>4</sup> In the case of neutrals we have seen that the effect of increasing nuclear charge was to initiate  $4f$  collapse by deepening the inner potential well. For a fixed  $Z$ , the effect of increasing ionization is to deepen the outer well of the effective potential curve. Thus the barrier between the two minima is lowered, from the outside this time rather than from the inside as in the case of increasing  $Z$ . Since increasing  $\zeta$ , the net core charge, enhances the  $4f$  wave-function contraction, one would expect that at a particular ion stage the  $4f$  electron will become more tightly bound than  $5p$  and, at a still higher stage, than  $5s$ . Curves of binding energy against  $\zeta$  will therefore intersect at or near particular ion stages and these intersections we will call, for simplicity, "crossing points."

To establish the crossing points from the existing spectroscopic data one must proceed indirectly. Thus in the Xe I isoelectronic sequence,<sup>6</sup> the resonance lines expected for a ground state  $5p^6\ ^1S$  are observed up to Ce V; some of these lines are observed for Pr VI but they could not be identified for Nd VII. According to Edlén<sup>7</sup> this is the result of the  $4f$  electron becoming more tightly bound than  $5p$  so that the ground configuration in the sequence changes from  $5p^6$  to  $4f^6$ . Looking now at increasing ion stages of praseodymium we note that they are known experimentally up to Pr V ( $5p^64f$ ). We have just seen that in Pr VI, because only some of the strong lines associated with a ground state  $5p^6$  configuration are observed, the  $4f$  and  $5p$  orbitals are showing incipient degeneracy. In going to Pr VII, because the core charge has increased, the  $4f$  electron is expected to be more tightly bound than  $5p$ , and the ground configuration would become  $4f^5$ .

Let us now consider "isoionic" sequences, that is, systems in which both the nuclear charge and total number of electrons increase so that the ion stage remains the same. The simplest example is that of the neutral atoms themselves. In this case when a subshell begins to fill it generally continues to do so until it is complete. Now consider the VII isoionic sequence. After Xe VII, the ground state of which is known experimentally to be  $4d^{10}5s^2$ , one might expect the configurations for Cs VII through Nd VII to be  $5s^25p$  through  $5s^25p^6$ . However, it has been seen already that the ground configuration of Pr VII is  $4f^5$ . Indeed at Ce VII the  $4f$  electron may be more tightly bound than  $5p$  and the ground configuration could possibly be  $4f^4$ . In this connection Reader and Ekberg<sup>6</sup> remarked that in Ce VI the  $5p^44f$  configuration is expected to be not far above the ground configuration  $5p^5$ . In any event, once the  $4f$  crossing has occurred in the isoionic sequence at Pr VII, one can expect on this simple picture that the  $4f$  shell will continue to fill until Er VII is reached with  $5s^24f^{14}$ . Past Er VII the ground-state configurations would then be of the form  $5s^24f^{14}5p^l$ . When W VII is reached, the  $5p$  subshell is full, and the relative  $4f$  and  $5p$  binding energies are no longer relevant in determining ground configurations. Some evidence on the  $4f$ - $5p$  energy trends is afforded by the behavior of the  $5p^55d$  and  $4f^{13}5d$  excited configurations in the Yb III isoelectronic sequence, which were shown by Sugar and Kaufman<sup>8</sup> to cross very near W VII. These authors also remarked that  $4f^{13}5p^6$  rather than  $4f^{14}5p^5$  is the more likely configuration for

TABLE I. Proposed working table of ground-state configurations<sup>a</sup> of ions in stages I—XVI for elements lanthanum through hafnium.

	I	II	III	IV	V	VI	VII	VIII	IX	X	XI	XII	XIII	XIV	XV	XVI
La	$5p^6 5d 6s^2$	$5p^6 5d^2$	$5p^6 5d$	$5s^2 5p^6$	$5s^2 5p^5$	$5s^2 5p^4$	$5s^2 5p^3$	$5s^2 5p^2$	$5s^2 5p$	$4d^{10} 5s^2$	$4d^{10} 5s$	$4d^{10}$	$4d^9$	$4d^8$	$4d^7$	$4d^6$
Ce	$5p^6 4f 5d 6s^2$	$5p^6 4f 5d^2$	$5p^6 4f^2$	$5p^6 4f$	$5s^2 5p^5$	$5s^2 5p^4$	$5s^2 4f^4$	$5s^2 4f^3$	$5s^2 4f^2$	$5s^2 4f$	$4d^{10} 5s^2$	$4d^{10} 5s$	$4d^{10}$	$4d^9$	$4d^8$	$4d^7$
Pr	$5p^6 4f^3 6s^2$	$5p^6 4f^3 6s$	$5p^6 4f^3$	$5p^6 4f^2$	$5s^2 5p^6$	$5s^2 4f^5$	$5s^2 4f^4$	$5s^2 4f^3$	$5s^2 4f^2$	$5s^2 4f$	$4d^{10} 5s^2$	$4d^{10} 5s$	$4d^{10}$	$4d^9$	$4d^8$	$4d^7$
Nd	$5p^6 4f^4 6s^2$	$5p^6 4f^4 6s$	$5p^6 4f^4$	$5p^6 4f^3$	$5s^2 5p^6$	$5s^2 4f^6$	$5s^2 4f^5$	$5s^2 4f^4$	$5s^2 4f^3$	$5s^2 4f^2$	$4d^{10} 5s^2$	$4d^{10} 5s$	$4d^{10}$	$4d^9$	$4d^8$	$4d^7$
Pm	$5p^6 4f^5 6s^2$	$5p^6 4f^5 6s$	$5p^6 4f^5$	$5p^6 4f^4$	$5p^6 4f^3$	$5s^2 4f^7$	$5s^2 4f^6$	$5s^2 4f^5$	$5s^2 4f^4$	$5s^2 4f^3$	$4d^{10} 5s^2$	$4d^{10} 5s$	$4d^{10}$	$4d^9$	$4d^8$	$4d^7$
Sm	$5p^6 4f^6 6s^2$	$5p^6 4f^6 6s$	$5p^6 4f^6$	$5p^6 4f^5$	$5p^6 4f^4$	$5s^2 4f^8$	$5s^2 4f^7$	$5s^2 4f^6$	$5s^2 4f^5$	$5s^2 4f^4$	$4d^{10} 5s^2$	$4d^{10} 5s$	$4d^{10}$	$4d^9$	$4d^8$	$4d^7$
Eu	$5p^6 4f^7 6s^2$	$5p^6 4f^7 6s$	$5p^6 4f^7$	$5p^6 4f^6$	$5p^6 4f^5$	$5s^2 4f^9$	$5s^2 4f^8$	$5s^2 4f^7$	$5s^2 4f^6$	$5s^2 4f^5$	$4d^{10} 5s^2$	$4d^{10} 5s$	$4d^{10}$	$4d^9$	$4d^8$	$4d^7$
Gd	$5p^6 4f^8 6s^2$	$5p^6 4f^8 6s$	$5p^6 4f^8$	$5p^6 4f^7$	$5p^6 4f^6$	$5s^2 4f^{10}$	$5s^2 4f^9$	$5s^2 4f^8$	$5s^2 4f^7$	$5s^2 4f^6$	$4d^{10} 5s^2$	$4d^{10} 5s$	$4d^{10}$	$4d^9$	$4d^8$	$4d^7$
Tb	$5p^6 4f^9 6s^2$	$5p^6 4f^9 6s$	$5p^6 4f^9$	$5p^6 4f^8$	$5p^6 4f^7$	$5s^2 4f^{11}$	$5s^2 4f^{10}$	$5s^2 4f^9$	$5s^2 4f^8$	$5s^2 4f^7$	$4d^{10} 5s^2$	$4d^{10} 5s$	$4d^{10}$	$4d^9$	$4d^8$	$4d^7$
Dy	$5p^6 4f^{10} 6s^2$	$5p^6 4f^{10} 6s$	$5p^6 4f^{10}$	$5p^6 4f^9$	$5p^6 4f^8$	$5s^2 4f^{12}$	$5s^2 4f^{11}$	$5s^2 4f^{10}$	$5s^2 4f^9$	$5s^2 4f^8$	$4d^{10} 5s^2$	$4d^{10} 5s$	$4d^{10}$	$4d^9$	$4d^8$	$4d^7$
Ho	$5p^6 4f^{11} 6s^2$	$5p^6 4f^{11} 6s$	$5p^6 4f^{11}$	$5p^6 4f^{10}$	$5p^6 4f^9$	$5s^2 4f^{13}$	$5s^2 4f^{12}$	$5s^2 4f^{11}$	$5s^2 4f^{10}$	$5s^2 4f^9$	$4d^{10} 5s^2$	$4d^{10} 5s$	$4d^{10}$	$4d^9$	$4d^8$	$4d^7$
Er	$5p^6 4f^{12} 6s^2$	$5p^6 4f^{12} 6s$	$5p^6 4f^{12}$	$5p^6 4f^{11}$	$5p^6 4f^{10}$	$5s^2 4f^{14}$	$5s^2 4f^{13}$	$5s^2 4f^{12}$	$5s^2 4f^{11}$	$5s^2 4f^{10}$	$4d^{10} 5s^2$	$4d^{10} 5s$	$4d^{10}$	$4d^9$	$4d^8$	$4d^7$
Tm	$5p^6 4f^{13} 6s^2$	$5p^6 4f^{13} 6s$	$5p^6 4f^{13}$	$5p^6 4f^{12}$	$5p^6 4f^{11}$	$4f^{14} 5p$	$4d^{10} 5s^2$	$4d^{10} 5s$	$4d^{10}$	$4d^9$	$4d^8$	$4d^7$				
Yb	$5p^6 4f^{14} 6s^2$	$5p^6 4f^{14} 6s$	$5p^6 4f^{14}$	$5p^6 4f^{13}$	$5p^6 4f^{12}$	$4f^{14} 5p^2$	$4f^{14} 5p$	$4f^{14} 5p$	$4f^{14} 5p$	$4f^{14} 5p$	$4d^{10} 5s^2$	$4d^{10} 5s$	$4d^{10}$	$4d^9$	$4d^8$	$4d^7$
Lu	$5p^6 5d 6s^2$	$5p^6 5d 6s$	$5p^6 6s$	$5p^6 6s$	$5p^6 4f^{13}$	$4f^{14} 5p^3$	$4f^{14} 5p^2$	$4f^{14} 5p$	$4f^{14} 5p$	$4f^{14} 5p$	$4d^{10} 5s^2$	$4d^{10} 5s$	$4d^{10}$	$4d^9$	$4d^8$	$4d^7$
Hf	$5p^6 5d^2 6s^2$	$5p^6 5d^2 6s$	$5p^6 5d 6s$	$5p^6 5d$	$5p^6 4f^{14}$	$4f^{14} 5p^4$	$4f^{14} 5p^3$	$4f^{14} 5p^2$	$4f^{14} 5p$	$4f^{14} 5p$	$4d^{10} 5s^2$	$4d^{10} 5s$	$4d^{10}$	$4d^9$	$4d^8$	$4d^7$

<sup>a</sup>Direct observations of ground configurations of free ions are available only for those elements to the left of the full line and for members of the silver and palladium isoelectronic sequence (excluding Pm xv and xvi) blocked out in the upper right-hand part of the table. The vertical double lines at the left and right show where the 4f energy is estimated to cross that of 5p and 5s, respectively. The central part of the table has a formal rather than a literal meaning because of the overlapping of low-lying configurations. (See text.)

<sup>b</sup>Derived from crystal spectra. (See Ref. 4.)

the ground state of W VIII.

In view of the above evidence it appears that the  $4f$ - $5p$  crossing occurs between the fifth and sixth ion stages (corresponding to the VI and VII spectra, respectively) from praseodymium (and very likely cerium) to hafnium. This behavior is indicated by the double vertical line in Table I. The phenomenon, even if there is some uncertainty as to its exact location, in all cases provides a striking example of the effect of ion stage on  $4f$  behavior.

With increasing ionization the  $4f$  electron, due to further contraction of its wave function, will eventually become more tightly bound than  $5s$ . Direct evidence for  $4f$ - $5s$  energy crossing is provided by the results of Even-Zohar and Fraenkel<sup>9</sup> and Sugar<sup>10</sup> on the Ag I isoelectronic sequence. Thus in going from Nd XIV to Sm XVI, as was shown by Sugar, the ground state changes from  $4d^{10}5s^2S$  to  $4d^{10}4f^2F$ . No further experimental evidence is currently available so that the stage at which the  $4f$ - $5s$  crossing occurs for a fixed  $Z$  value can be located with less assurance than in the case of  $4f$ - $5p$ . Cheng and Kim<sup>11</sup> have calculated the term values of all the low-lying states of  $4d^{10}nl$  with  $n=4$  and  $5$  for Ag I-like ions up to Th XLIV and predicted that  $4f$  becomes the ground state at Pm XV. Again on the assumption that with increasing  $Z$  the change in binding energy occurs at the same ion stage, the crossing of the  $4f$  and  $5s$  binding energies can be located between the XIV and XV stages; where this occurs is indicated by the double vertical line on the right-hand side of Table I.

It is now a simple matter to complete Table I by filling in the ground configurations for lanthanum to hafnium up to the XVI stage. The roster of configurations is, of course, not meant to be definitive and, in particular, it will be noted that in its preparation the tacit assumption was made that when  $5p$ - $4f$  crossing occurs, all  $5p$  electrons in a configuration are replaced by  $4f$ . Thus, near the crossing points the lowest configurations may, in fact, contain both  $4f$  and  $5p$  electrons, the  $5p$  subshell being only partially depopulated.

#### IV. TRENDS IN $4f$ AND $5p$ BINDING ENERGIES

Whereas the arguments in Sec. III indicate that the  $4f$  and  $5p$  orbitals become degenerate between the VI and VII spectra, we would like to know the relative energies of these orbitals as the ion stage increases. Since the  $4f$ - $5s$  crossing occurs at about the 14th stage and as the  $5s$ - $5p$  separation is ex-

pected to be fairly small, the  $4f$  energy must lie relatively close to the  $5p$  for a considerable range of ion stage. The most recent theoretical calculations of relevance are those of Fraga *et al.*<sup>12</sup> who calculated ionization potentials by the Hartree-Fock method up to the 11th stage. Using the Edlén isoelectronic formula<sup>13</sup> we extrapolated these data up to the 20th stage, and then plotted the results for each element as a function of ion stage. Two typical plots (for europium and terbium) are shown in Fig. 3.

It is seen from Fig. 3 that there is a sharp change in monotonic behavior at Eu X and Tb XII. These points correspond to the 10th and 12th members, respectively, of the Xe I isoelectronic sequence and the discontinuities arise because Fraga *et al.*<sup>12</sup> failed to take into account the change in ground-state configuration resulting from  $4f$ - $5p$  crossing, which occurs along this sequence at Nd VII. Hence, in Fig. 3 (and in similar plots for the other elements of interest) beyond the discontinuity the curves give the energy required to remove a  $5p$  rather than a  $4f$  electron, the latter of course corresponding to the correct ionization energy. For isoelectronic sequences beginning with the doubly ionized rare earths (i.e., La III, Ce III, etc.), Fraga *et al.* assumed  $4f^n$  ground configurations, and hence the regions of the plots below the discontinuities give the required  $4f$  ionization energy. An estimate of the  $4f$ - $5p$  separation as a function of ion stage can be obtained by extrapolating the lower part of the curve forwards and the higher part backwards. A further data point is furnished by the knowledge that the  $4f$ - $5p$  crossing point occurs near the seventh ion stage (see Sec. III). The results of the procedure are shown for europium and terbium in Fig. 4. Also shown is the trend of the  $5s$  energy estimated from the  $5s$  binding energy obtained by extrapolation of the Ag I isoelectronic sequence and from the  $4f$ - $5s$  crossing point which we have located at approximately the 14th ion stage. Figure 4 also includes the trend of the  $4d$  energy in europium determined from the  $4d$  ionization energy in the Pd I isoelectronic sequence (again extrapolated) and the  $4d$  energy in the neutral atom obtained from the x-ray spectrum.

It should be pointed out that prior to the work of Fraga *et al.* a table of calculated ionization energies of all elements in all stages was given by Carlson *et al.*<sup>14</sup> In this work a simple semiempirical shell model was used. The procedure, although sensitive to  $4f$  electron behavior, gave in each case the binding energy of the most loosely bound of

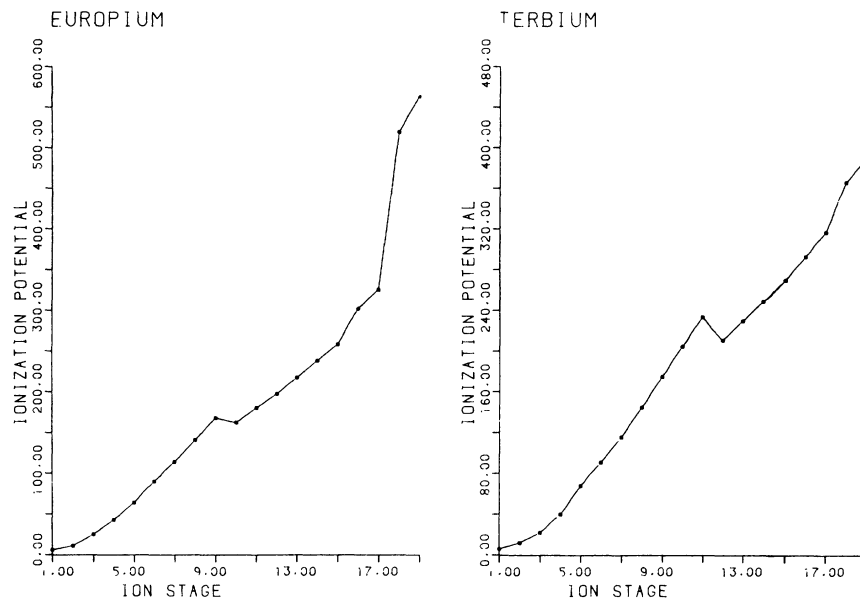


FIG. 3. Ionization potentials of different ion stages of europium and terbium. Experimental values are available only up to the fourth spectrum. For higher ion stages the experimental and theoretical values are extrapolated by applying Edlén's formula. Beyond the discontinuity, the graph gives the energy to remove a  $5p$  electron rather than the true ionization potential, which is the energy required to remove the more tightly bound  $4f$  electron (see text).

the  $4f$ ,  $5p$ , and  $5s$  electrons which, in many cases, did not correspond to the true ionization potential because the electronic rearrangement resulting from level crossing was not taken into account. Because of the closeness of the  $4f$ ,  $5p$ , and  $5s$  energies, however (see Fig. 4), the results were not grossly different from those extrapolated from the Hartree-Fock values. Carlson *et al.* did not specifically give ground-state configurations although such configurations could, in fact, be inferred from their data. On this basis we prepared another table analogous to Table I. The results predict that the  $4f$ - $5p$  crossing should occur between the IV and V

spectra instead of between the VI and VII which we have derived from the experimental data. Similarly the  $4f$ - $5s$  crossing would occur earlier than the available experimental results, i.e., as those on the palladium and silver isoelectronic sequences, would suggest. It is of interest to note that because the model of Carlson *et al.* was based on pure  $jj$  coupling a large  $5p$  spin splitting was introduced into the calculation and this, in turn, led to ground-state configurations with open  $5p$  subshells, the possibility of which was mentioned at the end of Sec. IV.

## V. INTERPRETATION OF EMISSION RESONANCES

With a knowledge of the ground state configurations given in Table I, it is possible to understand many of the features of the emission resonances observed in laser-produced plasmas involving elements from cesium to lutetium. We begin by consideration of the resonances observed when compound of the elements are used as target materials. Densitometer traces of some of these have already been presented in Fig. 2, which shows their evolution as a function of  $Z$ . Equilibrium considerations<sup>1</sup> predict that the radiating species are ions in stages VIII to XVI.

From general considerations the emission reso-

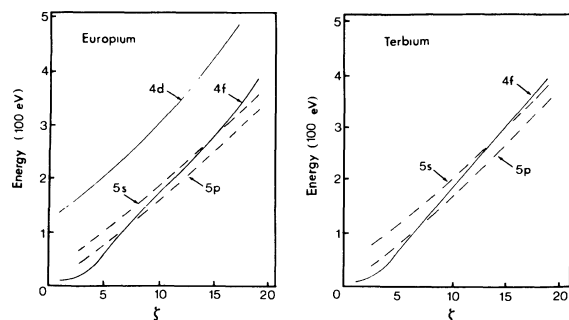


FIG. 4. The  $4f$ ,  $5s$ , and  $5p$  energies for europium and terbium as a function of core charge,  $\zeta$ , which is equivalent to ion stage in Fig. 3. In the case of europium the  $4d$  energy is also shown.

nances can be attributed to  $4d-4f$  transitions.<sup>1</sup> For the elements cesium, barium, and lanthanum the ion stages of interest (VIII—XVI) have ground configurations with either a full or partially filled  $d$  shell. (See Table I.) When  $d$  vacancies occur, the number of states can be considerable, while the presence of the  $f$  electron in combination with an unfilled  $d$  shell leads to a further degree of complexity. Thus, transitions of the type  $4d^k-4d^{k-1}4f$ , with which we are concerned, will generate a great number of lines; the predicted numbers for  $k=1-10$ , based on the assumption of  $LS$  coupling, are given in Table II. As the principal quantum number does not change (i.e.,  $\Delta n=0$ ), transitions from adjacent ion stages will tend to be superimposed and as ion stages from VIII to XVI are believed to contribute to the emission, a region of dense structure is expected. In general, for transitions between the more complex configurations such as  $4d^7-4d^64f$  (in Ba XV, for example), individual lines do not appear with any intensity because of the sharing of oscillator strength. For  $4d-4f$  transitions based on simpler ground configurations such as  $4d^{10}5s^25p$ ,  $4d^{10}5s^2$ ,  $4d^{10}5s$ ,  $4d^{10}$ , and  $4d^9$  (which in the case of barium would occur in the VIII—XII spectra), individual lines would be expected to appear strongly. Hence the overall structure would consist of a very large number of unresolved lines on which is superimposed a group of relatively strong well-defined lines. This is what, in fact, is observed. The fact that the resonances are so strong is clear evidence that in the ion stages of interest, the  $4f$  wave function in the excited configuration (no  $4f$  electrons occur in the ground states of cesium, barium, and lanthanum and their ions) is collapsed and hence yields a large oscillator strength because of the overlap with the  $4d$  wave function.

In going from cesium to lanthanum, some simplification of the spectrum and an increase in intensity of individual lines is observed as a result of the decreasing number of  $d$  vacancies in the ionization stages involved. This simplification is not maintained in cerium where the line density again increases and individual lines become less pro-

nounced. It is seen from Table I that cerium is the first lanthanide in which the  $4f$  electron becomes more tightly bound than  $5p$  in the ground configurations for some of the ionization stages of interest. Hence, the simplification resulting from  $4d$  filling is more than offset by the appearance of  $4f$  electrons in ground configurations. Table III gives the number of lines allowed by  $LS$  selection rules for transitions of the type  $4d^{10}4f^n-4d^94f^{n+1}$  for  $n=0-13$ . From these data and the relevant data in Table II it is easy to show that the number of lines predicted for cerium in stages VIII—XVI is 6585. In this connection the increasing complexity of the spectrum in going from lanthanum to cerium is itself further evidence of  $4f$  electrons in ground configurations of the latter.

As the number of  $4f$  electrons increases in the higher lanthanides beyond cerium a marked proliferation of levels occurs. To illustrate the evolution of the resulting resonances we plot in Fig. 5 the number of lines allowed in  $LS$  coupling for  $4d-4f$  transitions involving the ground states as given in Table I summed over the VIII—XVI spectra for the elements iodine to tungsten. The enormous increase in line numbers as the middle rare earths are approached should be noted. Beyond, say, europium all the ground configurations involved in the ion stages of interest are very complex and because of the sharing of oscillator strength no individual lines of even modest intensity are expected. This is fully in accord with the experimental observations which indicate that the resonances are made up of a region of continuum-like emission.

In fact the emission in the resonances is a good deal more complicated than the foregoing discussion would imply. It has been seen that after crossing, the  $4f$  and  $5p$  energies can be followed to higher ion stages and represented in graphs such as given in Fig. 4. The lines labeled  $5p$  and  $4f$  correspond to the average energies of the extreme configurations  $5p^l4f^{n-l}$  and  $4f^n$  (where  $l=6$  unless  $l+n < 6$ ) so that the average energies of intermediate configurations  $5p^{l-s}4f^{n-l+s}$  would be expected to correspond to points between these limits. Scru-

TABLE II. Numbers of lines predicted for  $4d^k-4d^{k-1}4f$  transitions in  $LS$  coupling.

$4d-4f$	3	$4d^6-4d^54f$	1894
$4d^2-4d4f$	39	$4d^7-4d^64f$	997
$4d^3-4d^24f$	250	$4d^8-4d^74f$	278
$4d^4-4d^34f$	910	$4d^9-4d^84f$	44
$4d^5-4d^44f$	1887	$4d^{10}-4d^94f$	1

TABLE III. Numbers of lines predicted for  $4d^{10}4f^n-4d^94f^{n+1}$  transitions in  $LS$  coupling.

$4d^{10}-4d^94f$	1	$4d^{10}4f^7-4d^94f^8$	75 997
$4d^{10}4f-4d^94f^2$	51	$4d^{10}4f^8-4d^94f^9$	48 151
$4d^{10}4f^2-4d^94f^3$	636	$4d^{10}4f^9-4d^94f^{10}$	19 483
$4d^{10}4f^3-4d^94f^4$	4 574	$4d^{10}4f^{10}-4d^94f^{11}$	4 317
$4d^{10}4f^4-4d^94f^5$	19 013	$4d^{10}4f^{11}-4d^94f^{12}$	638
$4d^{10}4f^5-4d^94f^6$	45 334	$4d^{10}4f^{12}-4d^94f^{13}$	53
$4d^{10}4f^6-4d^94f^7$	83 024	$4d^{10}4f^{13}-4d^94f^{14}$	3

tiny of the plots shows that the total spread in energy for our ion stages does not exceed 30 eV. We conclude therefore that the configurations  $5p^l4f^{n-l}$ ,  $l=1,2,3, \dots$ , lie close to and may even overlap the "ground" configuration  $4f^n$ . Indeed, as pointed out by Edlén<sup>13</sup> in the case of the  $d$  electrons in the transition elements, the definition of a ground configuration can be ambiguous and of limited significance.

Excitation of a  $4d$  electron generates a family of excited configurations  $4d^95p^l4f^{n-l+1}$  which again will be close together. Lines from the transitions  $4d^{10}5p^l4f^{n-l}-4d^95p^l4f^{n-l+1}$  for a range of  $l$  values are likely to contribute to the spectrum as

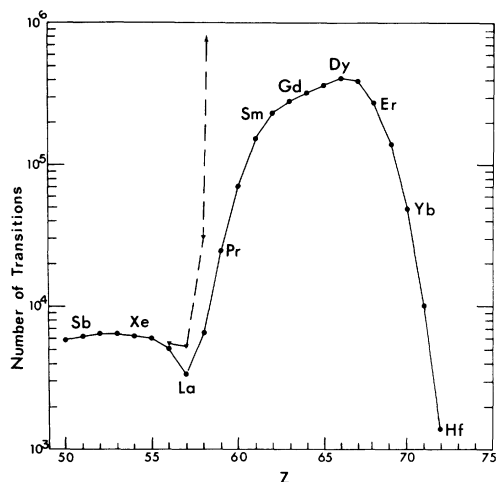


FIG. 5. Total numbers of lines in  $LS$  coupling predicted for  $4d \rightarrow 4f$  transitions summed over ion stages VIII—XVI. Full curve: Results based on ground configurations listed in Table I without inclusion of  $(4f,5p)-(4f,5s)$  degeneracy. Note the great number of lines towards the center of the sequence and the simplification predicted to occur at higher  $Z$ . Broken curve: Number of lines predicted when all possible low-lying configurations involving  $4f$ ,  $5p$ , and  $5s$  electrons are included (see text). Note in this case how the number of lines increases very rapidly past La. Furthermore, in this case no simplification is predicted as Hf is approached.

significantly as those of the  $4d^{10}4f^n-4d^94f^{n+1}$  already discussed. For example, in the relatively simple case of cerium, the inclusion of mixed  $4f,5p$  configurations increases the number of predicted  $4d-4f$  lines in the species Ce VIII to Ce XVI from 6585 to 30 622. For the higher lanthanides this number grows very rapidly (see Fig. 5). Furthermore cross transitions of the type  $4d^{10}5p^l4f^{n-l}-4d^95p^{l+1}4f^{n-l}$  will also occur although not with as high an intensity as the  $4d-4f$  transitions. As an example of the process, the manifold of configurations and the expected transitions for Gd XII are illustrated schematically in Fig. 6. In this figure, which is very qualitative, the configuration energies are shown as increasing slowly and monotonically with increasing  $5p$  occupancy, the total spread in the centroids of both high and low configurations being, as already pointed out, about 30 eV. The widths of the low-lying configurations are shown as relatively narrow (3 eV) because the  $4f-5p$  exchange interaction will be small. The high excited configurations, on the other hand, spread out to the extent of about 30 eV because of the large value of the  $4d-4f$  exchange integral.<sup>15</sup>

In the above discussion we have considered only the  $4f-5p$  proximity after the crossing point. An analogous effect is expected at and after the  $4f-5s$  crossing point where the configurations  $4f^n$ ,  $4f^{n-1}5s$ , and  $4f^{n-2}5s^2$  will lie close together. Here the further complication arises in that configurations of the form  $4f^{n-2}5s5p$ ,  $4f^{n-3}5s^25p$ , etc., can also play a role. In this connection it is of interest to note that, whereas we observed the resonance transition  $4d^{10}4f-4d^{10}5d$  of Sm XVI, no trace of the similar resonance doublet was found for Sm XIV whose ground configuration is given in Table I as  $4d^{10}5s^24f$ .

That many low-lying interacting configurations are involved as lower levels in the emission resonances can be inferred from our observations of the higher rare earths and the succeeding elements hafnium, tantalum, and tungsten. In the ion stages of interest, the spectra should, according to Table

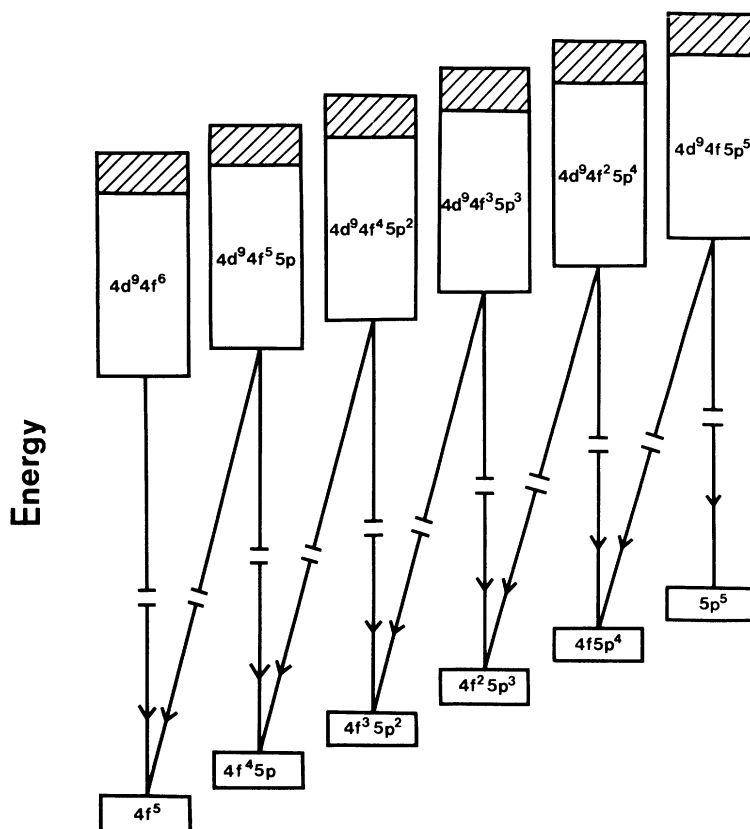


FIG. 6. Schematic representation of the relevant portion of the energy-level diagram of Gd XII and the expected transitions. As can be seen the latter will all lie in the same energy range. The hatched areas of the upper configurations indicate the approximate location of the levels which combine strongly with the lower configurations. The separation between the upper and lower configurations is  $\sim 100$  eV.

I, simplify as the  $f$  shell approaches completion (see also full line of Fig. 5). However, a scrutiny of the spectra for the  ${}^2D - {}^2F$  lines of the  $4d^{10}4f^{13} - 4d^9 4f^{14}$  transition in Hf XII, Ta XIII, and W XIV proved fruitless, which indicated that the large oscillator strength that would normally be associated with such simple transitions was, in fact, distributed over a considerable number of complex transitions of the type  $4d^{10}5p^1 4f^{13-l} - 4d^9 5p^l 4f^{14-l}$ .

#### VI. INTENSITIES AND WIDTHS OF RESONANCES

The considerable intensity of the resonances, to the almost complete exclusion of other features in the grazing incidence region, is of course to be attributed to the large overlap of the  $4d$  and the contracted  $4f$  wave functions. This overlap also gives rise to a large  $G^1(4d, 4f)$  exchange integral. At this stage the calculations of Sugar<sup>15</sup> on the  $4d-4f$  absorption spectra of the neutral lanthanides become relevant. Sugar considered the valence electrons to be inactive and the absorption to arise from the

doubly or triply ionized core. His procedure, which assumed that  $4f$  collapse was complete, required an arbitrary scaling down of the radial integrals. Subsequently Hansen,<sup>16</sup> Starace,<sup>17</sup> and Wendin<sup>18</sup> showed that  $4f$  collapse was not complete and that core-relaxation effects and collective phenomena should be taken into consideration in treating the neutral absorption. Since these effects reduce the value of the  $G^1$  integral and diminish with increasing ionization, Sugar's unscaled results should be applicable to the free ionized species. Therefore, we estimate that the width of an excited  $4d^9 4f^n$  configuration will be typically 30 eV. Since the resonances in the compounds (Fig. 2) extend over an energy interval of 9–18 eV they are too narrow to represent emission from the full range of an excited configuration. However, Sugar's approach predicts that most of the oscillator strength ( $f$  value) will arise from a fairly limited range of the upper energy levels, at the high energy end of the configuration. Our resonances, therefore, must correspond only to these high  $f$ -

value transitions. In Fig. 6 the hatched areas in the upper configurations indicate schematically the location of the levels of high oscillator strength. The weaker transitions which arise from the lower part of the configurations are, in general, not observed. Only when the core simplifies can some of the weaker lines be detected. For example, in Cs X to Nd XV the  $4d^{10}-4d^9 4f, {}^1S_0-{}^1P_1$  line lies within the region of resonance emission, while the  ${}^1S_0-{}^3P_1$  and  ${}^1S_0-{}^3D_1$  lines are observed at  $\sim 30$  eV to longer wavelengths.

One further aspect of intensities should be noted. It was observed that the overall strength of the resonances tended to decrease after  $Z=62$ . This is to be expected because Starace<sup>19</sup> has shown that the oscillator strength of the  $4d-4f$  transitions depends directly on the number of  $f$  vacancies in the upper state.

#### VII. COMPARISON OF SALT AND METAL SPECTRA; OPTICAL DEPTH EFFECTS

The resonances discussed in Secs. V and VI were emitted from plasmas in which the metal atoms were a minor constituent, comprising, in most instances, approximately 1% of the number density.<sup>1</sup> As already pointed out (Sec. II), the spectra from targets of the pure metals display substantial differences. As a specific example of the behavior of the lower- $Z$  elements, the spectra of lanthanum as observed from both salt and metal are shown again in Fig. 7, this time under greater enlargement and in a format suitable for comparison. It can be seen that, in the pure metal, the extent of the resonance is much greater than in the salt and consists of two regions of emission separated by a region of low intensity. For the lower- $Z$  elements from cesium to neodymium the metal spectra are relatively structured showing both emission and absorption lines, although as samarium is approached the appearance of the spectrum becomes more continuumlike. The continuum character is retained in the higher lanthanides although the overall intensity falls monotonically as lutetium is approached, so that the resonances tend to merge with the underlying recombination continuum. The net effect in the case of ytterbium, for example, is to give an essentially pure continuum from 40 Å, the limit of our observations, through the whole grazing incidence region, and indeed through the whole vacuum ultraviolet region to 2000 Å.<sup>3</sup>

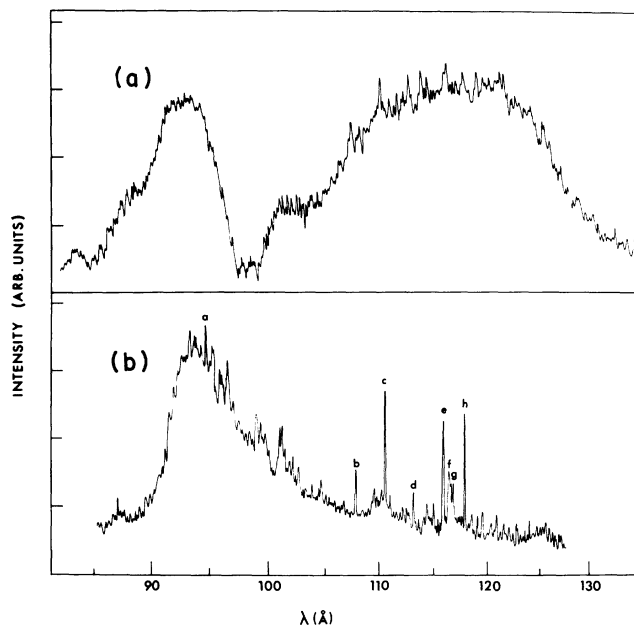


FIG. 7. Spectrum of lanthanum from laser-produced plasmas. (a) Target of lanthanum metal ( $\sim 100\%$  purity); (b) target of lanthanum oxide in araldite (lanthanum concentration  $\sim 1\%$ ). Line identifications: La XII,  $4d^{10}-4d^9 4f$ : (a)  ${}^1S_0-{}^1P_1$ , (d)  ${}^1S_0-{}^3D_1$ , (g)  ${}^1S_0-{}^3P_1$ ; La XII,  $4d^{10}-4d^9 5p$ , (b)  ${}^1S_0-{}^3D_1$ , (c)  ${}^1S_0-{}^1P_1$ . Impurity lines: O VI, (e) and (f); unidentified, (h).

The pronounced difference in the two types of resonance arises from the fact that in going from salt to pure metal the number density of the metal atoms of interest increases typically by a factor of 100 or more and, consequently, both the atomic emission and absorption in the plasma are radically altered.

In general, individual lines cannot be identified in our resonances because of their complexity, but the behavior of known lines in the simple spectra of the  $4d^{10}-4d^9 4f$  array, which has been observed from Cs X through Nd XV, may be used as a probe of plasma behavior. For this particular array, the  $f$  value of the  ${}^1S-{}^1P$  line, which can be taken as approximately 10, is greater than that of the weaker  ${}^1S-{}^3P$ ,  ${}^1S-{}^3D$  components by a factor lying within the range  $10^2-10^3$ .<sup>15</sup> Whereas the singlet line appears strongly in emission from salts containing the elements barium through praeceodymium, for the corresponding pure metals the transition appeared in absorption for barium through cerium. (It also occurred in absorption in the cesium salt, CsCl, used in our experiments, but here we are dealing with a rather optically thick system in which the number density of cesium was  $\sim 10\%$ ).

In Pr XIV it is completely self-absorbed and in Nd XV appears weakly in emission. In contrast, the low  $f$ -value components,  $^1S_0\text{-}^3P_1$  and  $^1S_0\text{-}^3D_1$ , appear in emission in both salts and metals and lie in the region of the longer wavelength intensity maximum.

For self-quenching, or line radiation trapping within Doppler broadened lines, we have the condition

$$\int_0^R n_{\xi}(r) dr > 9.28 \times 10^{15} \frac{kT_e^{1/2}}{Z} / f\lambda, \quad (1)$$

where  $n_{\xi}(r)$  is the number density of absorbing ions,  $r$  the radial coordinate,  $R$  the absorbing path length, and  $kT_e$  the plasma temperature (55 eV). Equation (1) is an integral form of Greim's<sup>20</sup> simplified expression for a homogeneous plasma. As mentioned, self-quenching of the  $^1S_0\text{-}^1P_1$  line of Pr XIV was observed in pure-metal plasmas yielding

$$\int_0^R n(\xi=14, r) dr = 10^{13} \text{ cm}^{-2}.$$

or a mean ion density,  $\bar{n}(\xi=14)$ , of  $2 \times 10^{14} \text{ cm}^{-3}$ . (In making this estimate  $R$  was taken as the radius of the plasma fireball, i.e.,  $\sim 0.5$  mm). For self-quenching of the  $^1S_0\text{-}^3P_1$  and  $^1S_0\text{-}^3D_1$  lines, the mean density required would be  $> 10^{16} \text{ cm}^{-3}$  and is not attained. In the elements with  $Z < 59$ , the  $^1S\text{-}^1P$  line, which now arises from species with  $\xi < 14$ , appears in absorption indicating that

$$\int_0^R n_{\xi}(r) dr > 10^{13} \text{ cm}^{-2}.$$

This corresponds to a mean ion density of roughly the same magnitude as before since the absorbing path,  $R$ , increases with decreasing  $\xi$  due to both recombination and decreased streaming rates. (As an example of the latter phenomenon, it was found that the  $2s\text{-}2p$  transitions of O III and the  $4f\text{-}5g$  doublet of Ce XII gave Doppler shifts consistent with expansion energies of 0.1 and 1 keV, respectively.)

The hundredfold decrease in ion densities encountered in proceeding from metal to salt plasmas gives  $\bar{n}_{\xi} \sim 10^{12} \text{ cm}^{-3}$  so that: (a) self-quenching and absorption become negligible and (b) the absolute emission rate is greatly reduced. Consequently the low oscillator strength transitions which occur at the long-wavelength region of the  $4d\text{-}4f$  array do not appear in the spectra (except in the special case already mentioned in which all of the energy

is concentrated in a few lines). On the other hand, radiation from transitions of high  $f$  value is transmitted through the plasma with only slight attenuation.

By contrast in the metal plasmas, the low  $f$ -value transitions at longer wavelength appear with good intensity and the full extent of the  $4d\text{-}4f$  array is manifested. Since ion densities of  $10^{16} - 10^{17} \text{ cm}^{-3}$  are required for self-absorption, these lines suffer negligible attenuation. For the high  $f$ -value transitions, however, the plasma becomes optically thick so that the intensity at the short-wavelengths end of the  $4d\text{-}4f$  array is greatly reduced. The radiation at the shortest wavelengths originates from the highest ion stages XV and XVI, which are effectively concentrated at small values of  $r$ , and these stages are not present in sufficient densities in the outer, cooler plasma regions to cause total self-absorption. Nevertheless, the magnitude of this absorption is sufficient to reduce the intensity to about that of the low  $f$ -value transitions at longer wavelengths.

The strongest attenuation will occur for the lower ion stages, which are numerous in the outer regions of the plasma and, consequently, correspond to large values of  $R$ . It is these ion stages which are believed to cause the strong absorption dip in the middle of the transition array. Indeed, in lanthanum the location of the minimum (102 Å) corresponds closely to the maximum in the absorption of the neutral vapor as observed by Radke.<sup>21</sup> Because of our plasma conditions, however, we do not expect neutral absorption to be of any great significance. Furthermore with increasing  $Z$  our absorption minima move away towards shorter wavelengths from those of Radke, indicating that in the plasmas significant absorption begins only at perhaps the third or fourth ion stage.

In the absorption minima of the lower  $Z$  spectra, in particular for cesium, barium, and to a lesser extent lanthanum, a considerable amount of line structure is evident. This can be attributed to the fact that the configurations involved are, in general, simpler than those encountered in the middle and higher lanthanides. In the latter case, absorption can arise from the many close or overlapping  $4f^n 5p^l$  configurations whose total energy span is expected to be considerably less than the average electron temperature and therefore will be populated under the conditions obtaining in our plasmas. Such a view is consistent with the observation that the absorption, like the emission becomes continuous for the middle and higher lanthanides.

## VIII. CONCLUSION

The ground-state configurations proposed in Table I enable the  $4d$ - $4f$  emission resonances for the elements from cesium to lutetium observed in plasmas of differing optical depths to be explained in a satisfactory, if qualitative, manner. In particular, the complexity of the spectra from cerium onwards is shown to be related to the role of  $4f$  electrons in the ground configurations of the ionic species which contribute to the emission. Hence, for a given  $Z$ , the effect of increasing ionization on the  $4f$  wave-function contraction is crucial. Once the  $4f$  binding energy crosses that of  $5p$ , a complex manifold of closely stacked low-lying configurations becomes the salient characteristic of the energy-level scheme. Indeed, which configuration provides the ground state cannot be established with certainty and, as mentioned, is a matter of limited significance. Thus, for example, although in Table I,  $4f^6$  is given as the ground configuration of Nd VII,  $4f^4 5p^2$ , or some other combination of  $4f$  and  $5p$  electrons may well generate the lowest state or be the configuration whose center of gravity is lowest. When configuration interaction is taken into consideration, such identifications become of even less significance. Our assumption of complete depopulation of the  $5p$  orbitals was made for simplicity and so the configurations in Table I beyond the sixth spectrum have a formal rather than a literal meaning. Indeed, in the table an alternative mode of assigning electrons to the  $5p$  and  $4f$  orbitals would be  $(5p4f)^q$ , where  $q$  is the number of electrons shared between the two orbitals; a

similar nomenclature for  $5s$  and  $4f$  electrons in the appropriate region of the table would be  $(5s4f)^r$ . The important point is that near the  $4f$ - $5p$  crossing and beyond we are in a domain where the character of the spectra is dominated by overlapping  $5p^{l-s} 4f^{n-l+s}$  configurations, where  $s$  varies from 0 to  $l$  (which usually is 6), and at higher ion stages by overlapping configurations involving  $4f$ ,  $5p$ , and  $5s$  electrons. In this region, which can be seen from Table I to extend over a considerable range of  $Z$  and ion stage, and in the adjoining regions of the table where the configurations contain a number of  $4f$  electrons, it would appear that the possibility of making a line and term analysis in the conventional sense would be out of the question. Even if a single ion species could be excited in isolation, its spectrum would be prohibitively complicated to permit such an analysis. With increasing ionization, of course, especially when all or nearly all of the  $4f$  electrons are removed, spectra of simple character will again appear.

## ACKNOWLEDGMENTS

This work was supported by the National Board of Science and Technology (Ireland) under research Grant No. URG/96/78. The latter portions of the work were also supported in part by the National Science Foundation under Grant No. PHY77-14953 to the University of Maryland. The authors are grateful to Drs. D. S. Ginter and M. L. Ginter for their helpful comments on the manuscript.

- <sup>1</sup>G. O'Sullivan and P. K. Carroll, *J. Opt. Soc. Am.* **71**, 227 (1981).  
<sup>2</sup>P. K. Carroll, E. T. Kennedy, and G. O'Sullivan, *Opt. Lett.* **2**, 72 (1978).  
<sup>3</sup>P. K. Carroll, E. T. Kennedy, and G. O'Sullivan, *Appl. Opt.* **19**, 1454 (1980).  
<sup>4</sup>W. C. Martin, R. Zalubas, and Lucy Hagen, *Atomic Energy Levels, the Rare Earth Elements* (Nat'l. Bur. Stand. U. S. NSRDS-NBS No. 60, 1978).  
<sup>5</sup>U. Fano and J. W. Cooper, *Rev. Mod. Phys.* **40**, 441 (1968); J. P. Connerade, *Contemp. Phys.* **19**, 415 (1978).  
<sup>6</sup>J. Reader and J. O. Ekberg, *J. Opt. Soc. Am.* **62**, 464 (1972).  
<sup>7</sup>B. Edlén, *Phys. Scr.* **7**, 93 (1973).  
<sup>8</sup>J. Sugar and V. Kaufman, *Phys. Rev. A* **12**, 994 (1975).  
<sup>9</sup>M. Even-Zohar and B. S. Fraenkel, *J. Phys. B* **5**, 1596 (1972).

- <sup>10</sup>J. Sugar, *J. Opt. Soc. Am.* **67**, 1518 (1977).  
<sup>11</sup>K. T. Cheng and Y. K. Kim, *J. Opt. Soc. Am.* **69**, 125 (1979).  
<sup>12</sup>S. Fraga, J. Kerwowski, and K. M. S. Saxena, *Handbook of Atomic Data* (Elsevier, Amsterdam, 1976).  
<sup>13</sup>B. Edlén, *Atomic Spectra, Handbuch der Physik*, **XXVII** (Springer-Verlag, Berlin, 1964), pp. 80–220.  
<sup>14</sup>T. A. Carlson, C. W. Nestor, N. Wasserman, and J. D. McDowell, *At. Data* **2**, 63 (1970).  
<sup>15</sup>J. Sugar, *Phys. Rev. B* **5**, 1785 (1972).  
<sup>16</sup>J. E. Hansen, *J. Phys. B* **5**, 1096 (1973).  
<sup>17</sup>A. F. Starace, *J. Phys. B* **7**, 14 (1974).  
<sup>18</sup>G. Wendin, *J. Phys. B* **9**, L297 (1976).  
<sup>19</sup>A. F. Starace, *Phys. Rev. B* **5**, 1773 (1972).  
<sup>20</sup>H. R. Griem, *Plasma Spectroscopy* (McGraw-Hill, New York, 1964).  
<sup>21</sup>E. R. Radke, *J. Phys. B* **12**, L71 (1979).